Vehicle System Dynamics

International Journal of Vehicle Mechanics and Mobility

ISSN: 0042-3114 (Print) 1744-5159 (Online) Journal homepage: https://www.tandfonline.com/loi/nvsd20

Stability enhancement of a high-speed train bogie using active mass inertial actuators

Yuan Yao, Guang Li, Yousef Sardahi & Jian-Qiao Sun

VEHICLE SYSTEM DYNAMICS
2019, VOL. 57, NO. 3, 389–407
https://doi.org/10.1080/00423114.2018.1469776

Stability enhancement of a high-speed train bogie using active mass inertial actuators

Yuan Yao[a,b], Guang Li[a], Yousef Sardahi[c] and Jian-Qiao Sun[d]

[a]State Key Laboratory of Traction Power, Southwest JiaoTong University, Chengdu, People's Republic of China; [b]State Key Laboratory of Heavy Duty AC Drive Electric Locomotive Systems Integration, Changsha, People's Republic of China; [c]College of Information Technology & Engineering, Marshall University, Huntington, WV, USA; [d]School of Engineering, University of California, Merced, CA, USA

ABSTRACT

In this study, a method regarding frame lateral vibration control based on the state feedback of an additional oscillator is proposed, so as to improve the bogie hunting stability. The multi-objective optimisation method (MOOP), with two objective functions of the stability index and control effort, is solved by the NSGA-II algorithm to obtain the feedback gains. The frame lateral vibration control can effectively improve the bogie hunting stability according to the linear and nonlinear analysis of a high-speed train bogie, in which a fault of the yaw damper and time delay in the control system are considered. The effect of the oscillator suspension parameters and time delay on the system stability and robustness are analysed. The results show that the damped vibration frequency of the oscillator should be equal to the bogie hunting frequency, but a harder oscillator suspension can be used to improve the hunting critical speed margin of the bogie control system. However, just as how the feeding the frame states back directly, a hard oscillator suspension will lead to instability in the control system at a certain time delay. Therefore, the improvement of bogie hunting stability and reduction of control system stability must be considered when optimising the oscillator parameters. For the 350 km/h train bogie covered in this study, the optimal mass, natural frequency and damping ratio of the additional oscillator are acquired.

ARTICLE HISTORY
Received 6 November 2017
Revised 17 March 2018
Accepted 18 April 2018

KEYWORDS
High-speed train bogie; hunting stability; active control; time delay; multi-objective optimisation; finite dimensional state space approximation

1. Introduction

The application of active controls to railway vehicles has garnered increasing attention in recent years. Most of the research concerns tilting train control and the secondary suspension semi-active or active control, in order to enhance the vehicle lateral and vertical smoothness for greater ride comfort, and to reduce high-frequency elastic vibration in the car body [1,2]. As the effects of bogie primary suspension on the critical velocity of railway vehicles have been thoroughly studied, researchers have proposed the use of semi-active and full-active suspension control to improve the lateral stability of the train [3–10]. Many different approaches for active primary suspensions have been reported in previous studies

CONTACT Jian-Qiao Sun jqsun@ucmerced.edu

[11]. The lateral stability of train employing inerters suspension has been investigated and the inerters are deemed effective in improving the lateral stability [12–14]. Feedback control systems can be applied either directly or indirectly [15]. The direct control involves the application of an actuator onto a solid wheelset or axle with independently rotating wheels. A practical compromise is to indirectly apply a yaw torque at the secondary suspension level, a concept known as 'Secondary Yaw Control' (SYC). The actuators may be designed to replace the traditional passive yaw dampers, so that active control of the running gear can be introduced without a substantial redesign of the bogie, which signifies that radical simplifications of the vehicle design may be limited [16].

In the active control design for trains, the lateral hunting stability of railway vehicles at high speed is one of the greatest dynamic problems, in which the conflict between the hunting stability and curving performance is well known [17]. When the vehicle runs on poor tracks or in a poor operating environment, the suspension performances may change during service, due to tread wear and component failure. Loss of the lateral stability causes poor ride comfort and even derailing accidents. Active control of high speed trains is a great alternative to passive methods, because of their flexibility. There has been a great number of studies regarding the use of active control onto the solid wheelset or independently rotating the wheel to improve the stability of the bogie or wheelset, while the control scheme has also been used to improve the curving performance [18–20]. However, the direct application of active control onto wheelsets to improve the running stability still faces challenges in practice.

In the present study, the authors presented an indirect method for improving the bogie hunting stability, by means of controlling the frame lateral vibration with the motor active flexible suspension of a high-speed train bogie [21]. The control is effective in improving the hunting stability. However, the time delay is harmful toward the stability of the bogie control system, particularly when the control acting on the frame is calculated based on the linear feedback of the frame states. The frame lateral vibration control is practical and low risk. In this paper, with the purpose of reducing the influence of delay on the stability of the bogie control system, the frame lateral vibration control with the state feedback of an additional oscillator is proposed. A linear dynamic model of a 350-km/h train bogie with a faulty yaw damper and time delay in the control system is taken as an example and is presented in Section 2. A multi-objective optimisation problem (MOOP) with two objective functions of the stability index and the control effort in terms of the feedback gains is presented in Section 3 and is solved using the NSGA-II algorithm. The effects of the oscillator suspension parameters and time delay on the system stability and robustness are analysed. Finally, the non-linear stability and time domain responses of the bogie control system are analysed to verify the control design.

2. Active control of frame lateral vibration

2.1. Bogie linear model

In this study, the wheelset movement is indirectly controlled by controlling the frame lateral vibration, so as to improve the hunting stability. The active control efforts acting on the frame are based on the feedback states of two additional oscillators fixed on the frame. Two mass inertial actuators, respectively, mounted on the front- and rear end beams, are used to

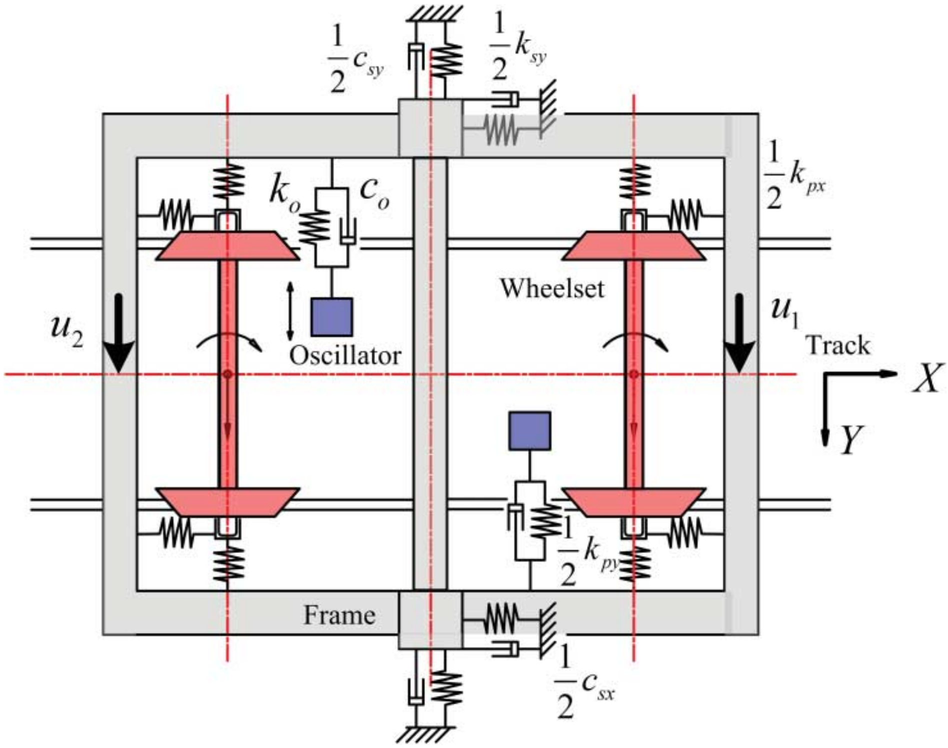

Figure 1. The bogie model with the additional oscillator.

exert the lateral vibration control. The simplified model of this system is shown in Figure 1. This model describes a lateral movement of a two-axle bogie. We assume that the lateral position of the car body is pre-determined, and that the bogie frame is connected with a fixed coordinate system through the secondary suspension, such as a spring and damper in the longitudinal and lateral directions. The bogie has two solid axle wheelsets, which are attached to the bogie frame via suspension springs in the longitudinal and lateral directions. The additional oscillator is connected to the side beam of the frame by the elastic and damping elements. The frame and wheelset in the model have lateral and yaw degrees of freedom, while the oscillator has only a lateral degree of freedom. The dynamic model was found to have five rigid bodies and eight degrees of freedom. The model describes the lateral movements of the bogie and reads,

$$\mathbf{M}_b\ddot{\mathbf{y}} + \mathbf{C}_b\dot{\mathbf{y}} + \mathbf{K}_b\dot{\mathbf{y}} + = \mathbf{q} + \mathbf{E}\mathbf{u} + \mathbf{w}d(t), \tag{1}$$

where $\mathbf{y} = [y_{w1}, \varphi_{w1}, y_{w2}, \varphi_{w2}, y_f, \varphi_f, y_{o1}, y_{o2}]^{\mathrm{T}}$. The states y_{w1}, y_{w2}, y_f, y_{o1} and y_{o2} are the lateral displacements of wheelset 1, wheelset 2, frame, oscillator 1 and oscillator 2, respectively. φ_{w1}, φ_{w2} and φ_f represent the yaw angles of wheelset 1, wheelset 2 and frame. $\mathbf{M}_b$, $\mathbf{C}_b$ and $\mathbf{K}_b$ are the mass, damping and stiffness matrices of the bogie system. $\mathbf{q} = -\mathbf{K}_r\mathbf{y} - \mathbf{C}_r\dot{\mathbf{y}}$ represents the wheel–rail interaction forces under the assumption that the spin creep forces of the wheelset are negligible. The elements of the matrices $\mathbf{K}_r$ and $\mathbf{C}_r$ are listed in the appendix. The total stiffness matrix $\mathbf{K} = \mathbf{K}_b + \mathbf{K}_r$ of the system is non-symmetrical because $\mathbf{K}_r$ is asymmetric stiffness. The off-diagonal elements of $\mathbf{K}_r$ represent the coupling of the wheelset lateral and yaw movements caused by the interaction of wheel and rail in the tangential direction, which inputs energy into the system and is responsible for the unstable hunting motion of the high-speed train. The total system damping matrix $\mathbf{C} = \mathbf{C}_b + \mathbf{C}_r$ is symmetrical. $\mathbf{C}_r$ is related to the speed v. As v increases, the damping decreases. In a period of hunting motion, if the input and the consumed energy of the bogie are equal, the linear system is in the critical stability state. The corresponding v is the linear critical speed. $\mathbf{u} = [u_1, u_2]^{\mathrm{T}}$ is a vector of the lateral active control forces applied on the bogie frame by two inertial actuators located on the front and rear beams, respectively. $\mathbf{E}$ is the control influence matrix. These matrices and vectors are listed in the appendix. The values and definitions of system parameters are listed in reference [21]. In order to study the effects of active control on improving the bogie hunting stability, the damping of yaw damper is chosen to be one fourth of its design value such that the bogie is in a faulty state. The vector $\mathbf{w}$ is defined as $\mathbf{w} = [k_{py}, 0, k_{py}, 0, 0, 0, 0, 0]^{\mathrm{T}}$. $d(t)$ is the external disturbance on the wheelsets due to, for example, track irregularity.

2.2. State equation

The state equation of the system can be written as follows [21]:

$$\dot{\mathbf{x}}(t) = \mathbf{A}\mathbf{x}(t) + \mathbf{B}\mathbf{u}(t) + \mathbf{F}\mathrm{d}(t), \tag{2}$$

where the state vector is defined as

$$\mathbf{x} = [y_{w_1}, \varphi_{w_1}, y_{w_2}, \varphi_{w_2}, y_f, \varphi_f, y_{o_1}, y_{o2}, \dot{y}_{w_1}, \dot{\varphi}_{w_1}, \dot{y}_{w_2}, \dot{\varphi}_{w_2}, \dot{y}_f, \dot{\varphi}_f, \dot{y}_{o_1}, \dot{y}_{o2}]^{\mathrm{T}}. \tag{3}$$

The system matrices $\mathbf{A}$ and $\mathbf{B}$, and the vector $\mathbf{F}$ are given by

$$\mathbf{A} = \begin{bmatrix} \mathbf{0}_{8\times 8} & \mathbf{I}_{8\times 8} \\ -\mathbf{M}^{-1}\mathbf{K} & -\mathbf{M}^{-1}\mathbf{C} \end{bmatrix}, \tag{4}$$

$$\mathbf{B} = \begin{bmatrix} \mathbf{0}_{8\times 2} \\ \mathbf{M}^{-1}\mathbf{E} \end{bmatrix}, \quad \mathbf{F} = \begin{bmatrix} \mathbf{0}_{8\times 1} \\ \mathbf{M}^{-1}\mathbf{w} \end{bmatrix}. \tag{5}$$

In this study, the control forces are applied to the frame to indirectly influence the motion of the wheelset. The bogie control system is under-actuated [22]. We consider a state feedback control of a subsystem, which consists of the frame and two oscillators. The subsystem has eight state variables. We then rearrange the order of the state variables in Equation (3) as follows:

$$\mathbf{x}_N = \begin{bmatrix} \mathbf{x}_{N1} \\ \mathbf{x}_{N2} \end{bmatrix}, \tag{6}$$

where $\mathbf{x}_{N1} = [y_f, \varphi_f, y_{o_1}, y_{o_2}, \dot{y}_f, \dot{\varphi}_f, \dot{y}_{o_1}, \dot{y}_{o_2}]^{\mathrm{T}}$ and $\mathbf{x}_{N2} = [y_{w_1}, \varphi_{w_1}, y_{w_2}, \varphi_{w_2}, \dot{y}_{w_1}, \dot{\varphi}_{w_1}, \dot{y}_{w_2}, \dot{\varphi}_{w_2}]^{\mathrm{T}}$. $\mathbf{x}_{N1}$ denotes the state variables of the subsystem.

Let $\mathbf{T}$ be a matrix that transforms the state vector $\mathbf{x}$ into the new one, in which $\mathbf{x}_N(t) = \mathbf{T}\mathbf{x}(t)$. The matrices and vectors of the transformed system are given by

$$\mathbf{A}_N = \mathbf{T}\mathbf{A}\mathbf{T}^{-1} = \begin{bmatrix} \mathbf{A}_{N11} & \mathbf{A}_{N12} \\ \mathbf{A}_{N21} & \mathbf{A}_{N22} \end{bmatrix},$$

$$\mathbf{B}_N = \mathbf{TB} = \begin{bmatrix} \mathbf{B}_{N1} \\ \mathbf{0}_{8\times 2} \end{bmatrix}, \quad \mathbf{F}_N = \mathbf{TF} = \begin{bmatrix} \mathbf{0}_{8\times 1} \\ \mathbf{F}_{N2} \end{bmatrix}. \tag{7}$$

The state equation for the subsystem reads

$$\begin{aligned} \dot{\mathbf{x}}_{N1} &= \mathbf{A}_{N11}\mathbf{x}_{N1}(t) + \mathbf{A}_{N12}\mathbf{x}_{N2}(t) + \mathbf{B}_{N1}\mathbf{u}(t), \\ \mathbf{z}(t) &= \mathbf{D}\mathbf{x}_{N1}(t), \end{aligned} \tag{8}$$

where $\mathbf{D}$ is the output matrix for the subsystem and is listed in the appendix. It can be determined that $(\mathbf{A}_{N11}, \mathbf{B}_{N1})$ is controllable. $\mathbf{A}_{N12}\mathbf{x}_{N2}(t)$ acts as a disturbance to the subsystem.

Consider an output feedback control $\mathbf{u} = -\mathbf{K}_c\mathbf{z}(t)$, where $\mathbf{K}_c$ is the feedback gain matrix. We choose the relative displacement from the oscillator mass to the installation point on the frame, and the lateral absolute velocity of oscillator mass as the output $\mathbf{z}$ is defined as

$$\mathbf{z} = [y_{o_1} - (y_f + L_o\varphi_f), y_{o_2} - (y_f - L_o\varphi_f), \dot{y}_{o_1}, \dot{y}_{o_2}]^{\mathrm{T}}. \tag{9}$$

Using this control law, the closed-loop dynamic matrix of the system reads

$$\mathbf{A}_{cl} = \mathbf{A}_N - \mathbf{B}_N[\mathbf{K}_c \quad 0]. \tag{10}$$

We have found that when a control gain $\mathbf{K}_c$ is selected to stabilise subsystem (8), the overall closed-loop system $\mathbf{A}_{cl}$ is also stable. Nevertheless, the stability of the closed-loop system places a constraint on the control design. Aside from the stability of the closed-loop system, the stability margin and energy efficiency of the controller should also be considered in the design. These requirements will be set up and defined in Section 3.

For the motion equation of a single wheelset with an elastic primary suspension, the lateral and yaw movement of the wheelset are coupled by the wheel–rail tangential forces. The lateral and yaw frequencies of the wheelset are the same, while their phase angles are different. The expression of lateral stiffness k_o and damping c_o of the oscillator suspension are defined as follows:

$$\begin{aligned} k_o &= (2\pi f_o)^2 m_o, \\ c_o &= 2\xi_o m_o(2\pi f_o), \end{aligned} \tag{11}$$

where f_o is the oscillator natural frequency in Hz. It is also known as the oscillator suspension frequency. ξ_o is the oscillator damping ratio, and m_o is the mass of oscillator in kg.

3. Multi-objective optimal control

3.1. Multi-objective optimal control design

A multi-objective optimisation based on genetic algorithm is adopted to optimise the control gain and oscillator suspension parameters. We consider the gain $\mathbf{K}_c = [k_1, \ldots, k_n]$ as the design parameters for the system discussed in Section 2. The states of relative displacement to the installation point and lateral absolute velocity of the oscillator mass are fed back, and the control gains of the two actuators at the two ends of the frame are different. Therefore, n is 4. The system stability margin and energy efficiency of the controller are the objectives of the control design. The multi-objective optimal design problem is stated as

$$\min\left\{\zeta_{\max}, \mathbf{K}_c^{\mathrm{T}}\mathbf{K}_c\right\}, \tag{12}$$

where $\zeta_{\max}$ denotes the maximum ratio between the real part and the modulus of eigenvalues of the matrix $\mathbf{A}_{cl}$ defined in Equation (10), and describes the stability margin of linear systems (a negative sign indicates a stable system). The term $\mathbf{K}_c^{\mathrm{T}}\mathbf{K}_c$ denotes the Frobenius norm of the control gain matrix $\mathbf{K}_c$. Due to the fact that the control system is optimised for zero initial conditions, the control effort cannot be included directly in the objective space, and its Frobenius norm is used instead. By minimising this norm, the total control energy is also minimised.

The NSGA-II algorithm is used to solve the MOOP. Most of the default settings of the algorithm are retained, with only two parameters being changed, namely population size and generation number. In this study, the population size is set to 500, and the number of generation is set to 1000.

3.2. Multi-objective optimal control results

First, the optimal oscillator suspension parameters are designed. We consider the objective $\zeta_{\max}$. The suspension frequency f_o and damping ratio ξ_o are used as the design parameters. The calculation range of f_o is from 0 to 10 Hz, and the range of ξ_o (a positive sign indicates a stable value) is 0 to 1. Figure 2 shows the maximum damping ratio $\zeta_{\max}$ of the bogie control system at different oscillator suspension parameters. In subgraphs (a) and (b), the mass of oscillator m_o is 10 and 850 kg, respectively. The latter is the weight of motor in the power bogie. The flexible suspension motor can be used instead of the additional oscillator in some motor bogies [23,24]. The results show that the influences of the suspension parameters on the system stability with the two types of mass are basically the same. The larger f_o and ξ_o are, the more stable the system will be. For the flexible suspension of the oscillator mass, the f_o and ξ_o respectively are set to 5 Hz and 0.5 in the following studies according to the optimisation results.

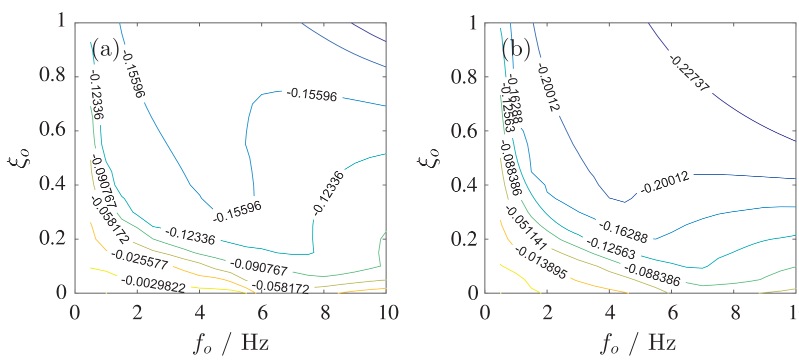

Figure 2. The contour of minimum $\zeta_{\max}$ that can be achieved by MOOP with different oscillator suspension parameters: (a) oscillator mass is 10 kg and (b) oscillator mass is 850 kg.

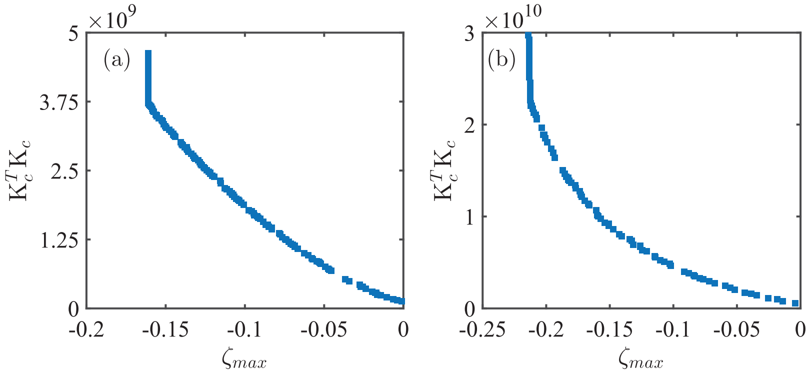

Figure 3. The Pareto front of MOOP: (a) the mass of oscillator is 10 kg and (b) the mass of oscillator is 850 kg.

Figure 3 shows the Pareto front of the bogie control system with the oscillator suspension parameters. The Pareto front illustrates a conflicting relationship between $\zeta_{\max}$ and $\mathbf{K}_c^{\mathrm{T}}\mathbf{K}_c$. With the increase of control effort, the bogie gradually becomes more stable. However, the system stability cannot be increased infinitely with the increasing of control effort, and the minimum $\zeta_{\max}$ are -0.16 and -0.21 at the two types of mass. This is due to the fact that the frame vibration modal damping determines the minimum $\zeta_{\max}$, according to the root locus analysis in Section 5. The Pareto front highlights the importance of the MOOP design. By having different design options, the decision maker can choose any point from the solution set which meets the performance requirements. It may be seen from the figures that the bogie linear model with a fault of yaw damper is in a critical stable state before applying the control at the speed of 350 km/h, and the active control can effectively improve the system stability. The $\zeta_{\max}$ is preset to be $\zeta_{\mathrm{set}} = -0.15$, so as to determine the feedback gain from the Pareto set. In some cases, the minimum $\zeta_{\max}$ of the system with optimal

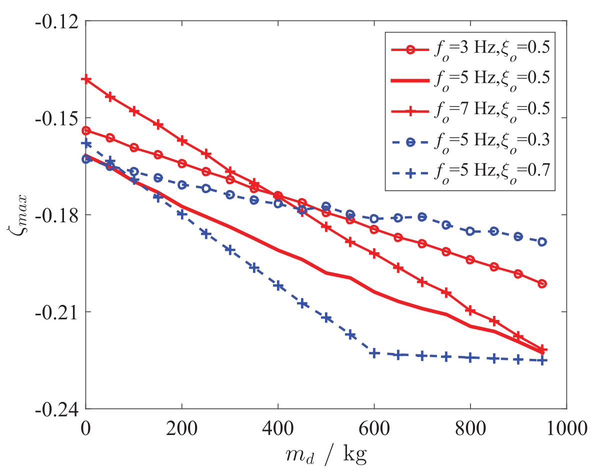

Figure 4. The effect of oscillator mass on the system stability with different oscillator suspension parameters.

gains is calculated by MOOP larger than −0.15. We choose the preset values ζ_{set}, so that

$$\zeta_{set} = \max\{\min(\zeta_{max}), -0.15\}. \tag{13}$$

Figure 4 shows the influences of m_o on the minimum ζ_{max} for different oscillator suspension parameters. We can conclude that a greater oscillator mass is beneficial to improving the system stability, especially with a harder oscillator suspension. The oscillator mass may be that of the suspended motor. Moreover, the mass and suspension parameters of the oscillator affect the vibration frequency and phase relative to the frame, and subsequently the frequency and phase of the active control force.

4. Time-delayed control

The time delay in the control changes the phase of the active control force and may negatively influence the control performance. In a feedback control system, time delay is inevitable. In this section, the influence of time delay in the control system on the bogie hunting stability is analysed using the continuous time approximation (CTA) method [21,25].

4.1. The stability analysis

It is quite easy to analyse the stability of a linear time delay system using the CTA method. In this study, the delayed part of the state vector is extended to 20 points, and the feedback gains are selected based on the ζ_{set} in Equation (13). The effects of time delay with different oscillator parameters and bogie running speeds on the system stability are discussed in the present section. Figure 5 shows the calculated maximum damping ratio ζ_{max} by MOOP versus time delay τ at different oscillator mass and running speeds. f_o and ξ_o are assumed as 5 Hz and 0.5 to achieve these results. Subgraphs (a), (b) and (c) are the results at speeds of 200, 350 and 500 km/h, respectively. At speeds below 350 km/h, the ζ_{max} of the system basically equals ζ_{set} when the τ is less than 1 ms. When τ is about 15 ms, a small oscillator mass will reduce the system stability, especially in a low-speed range. At the speed of 500 km/h, due to the function of vibration absorbing, the system stability with

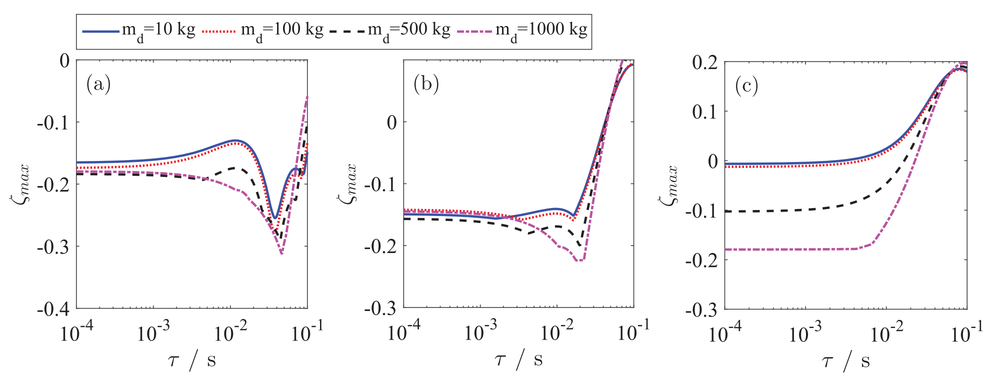

Figure 5. The effect of time delay on the system stability with different oscillator mass: (a) $v = 200$ km/h; (b) $v = 350$ km/h; (c) $v = 500$ km/h.

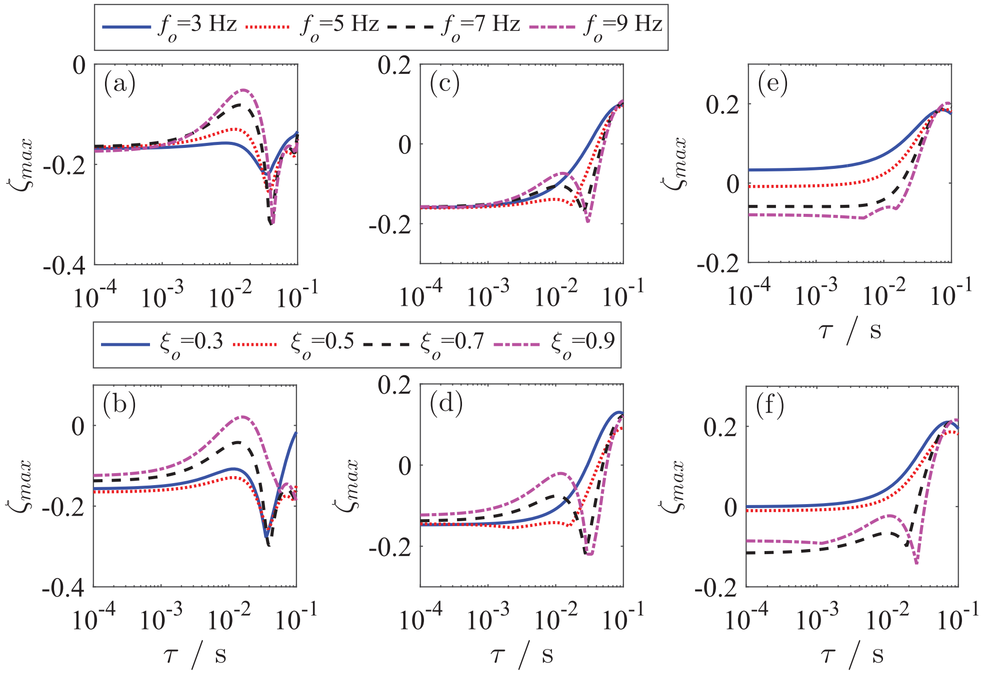

Figure 6. The effect of time delay on the system stability with different oscillator suspension parameters: (a) $v = 200$ km/h, $\xi_o = 0.5$; (b) $v = 200$ km/h, $f_o = 0.5$; (c) $v = 350$ km/h, $\xi_o = 0.5$; (d) $v = 350$ km/h, $f_o = 0.5$; (e) $v = 500$ km/h, $\xi_o = 0.5$; (f) $v = 500$ km/h, $f_o = 0.5$.

a large oscillator mass is much better than the system with a small oscillator mass when the τ is smaller than 100 ms. In general, a large oscillator mass is conducive to the system stability.

Figure 6 shows the calculated $\zeta_{\max}$ versus τ at different oscillator suspension parameters and running speeds. The oscillator mass m_d is designated as 10 kg to achieve these results. With the increase of τ, the $\zeta_{\max}$ increases and the system stability reduces, especially at 15 ms. The harder the oscillator suspension is, the more the stability reduces as the τ increases. However, the appropriate oscillator suspension parameters can reduce this phenomenon. That is the reason why using an additional oscillator to provide the feedback states but the bogie frame, yet using a hard oscillator suspension can improve the bogie hunting stability at high speeds, such as 500 km/h. For a bogie adopted in a 350-km/h train, the optimised oscillator suspension frequency f_o and damping ratio ξ_o are respectively set as 5 Hz and 0.5 in this study. With this oscillator suspension parameter set, the feedback gain values of the oscillator relative displacement and the absolute velocity are 1858 N/m and 40,630 N/m·s^{-1}, respectively, when the system maximum damping ratio $\zeta_{\max}$ is -0.15. With these suspension parameters and a mass of 10 kg, the delay below 20 ms basically has no effect on the system stability at the speed of 350 km/h, but it still reduces the stability, especially at 15 ms, when the speed is less than 350 km/h. Moreover, an appropriate time delay, such as 20–40 ms, can be used to improve the system stability at speeds below 350 km/h. Therefore, we can use the feedback delay to improve the Active Vibration Suppression [26].

4.2. Optimal oscillator suspension parameters

According to the analysis in Section 4.1, the time delay in the control system has a significant impact on the stability of the bogie control system. However, an appropriate oscillator suspension parameter is helpful to improving the system stability and counteracting the negative effects caused by delay. The delay of 15 ms is the most unfavourable, regardless of what the calculation condition is. In this section, the optimised oscillator suspension parameters are analysed to determine a better system stability at the delays of 0 and 15 ms, respectively. Figure 7 shows the contour of $\zeta_{\max}$ versus f_o and ξ_o. The oscillator mass is designated as 10 kg, and the ζ_{set} in Equation (13) is used to obtain the control gains. Subgraphs (a), (c) and (e) show the results with a delay of 0 ms at the speeds of 200, 350 and 500 km/h, respectively. Subgraphs (b), (d) and (f) show the results with a delay of 15 ms at the speeds of 200, 350 and 500 km/h, respectively. When there is no delay, the larger the f_o and ξ_o will be, the more stable the system is. However, if the delay of 15 ms is considered, a large f_o and ξ_o are harmful to the system stability, and the optimal suspension parameters will be different at different running speeds. The optimal f_o is about 3, 5 and 7 Hz at the speeds of 200, 350 and 500 km/h, respectively. The relationship between the optimal f_o and ξ_o resembles a hyperbola, in which the larger f_o is, the smaller the corresponding ξ_o is needed to be.

4.3. Robustness to system parameters

In order to investigate the dynamics performance of the bogie after applying active control, as well as the control robustness of the system with different oscillator suspension

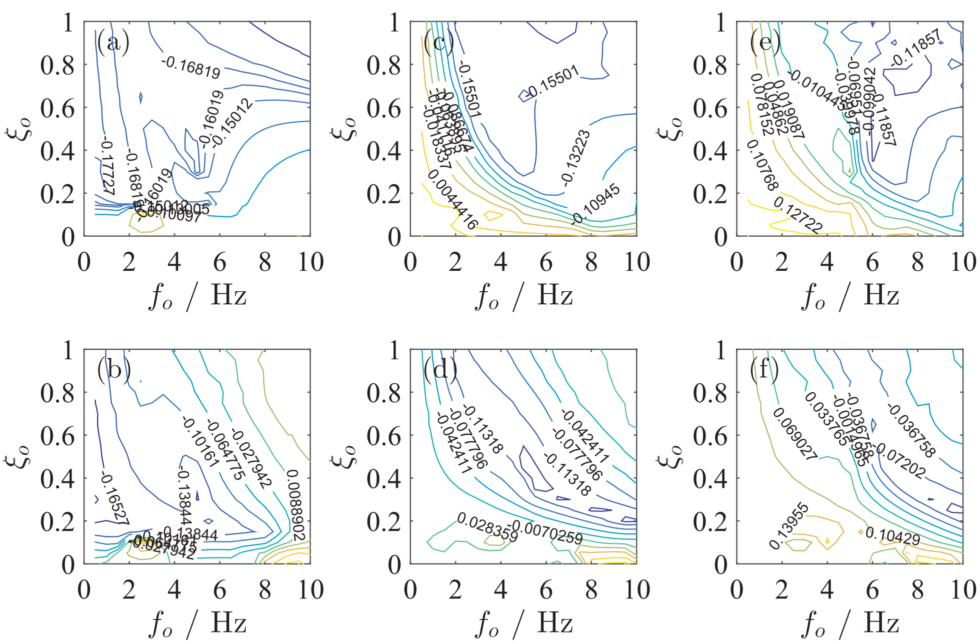

Figure 7. The optimal oscillator suspension parameters in different calculation conditions: (a) $v = 200$ km/h, $\tau = 0$ ms; (b) $v = 200$ km/h, $\tau = 15$ ms; (c) $v = 350$ km/h, $\tau = 0$ ms; (d) $v = 350$ km/h, $\tau = 15$ ms; (e) $v = 500$ km/h, $\tau = 0$ ms; (f) $v = 500$ km/h, $\tau = 15$ ms.

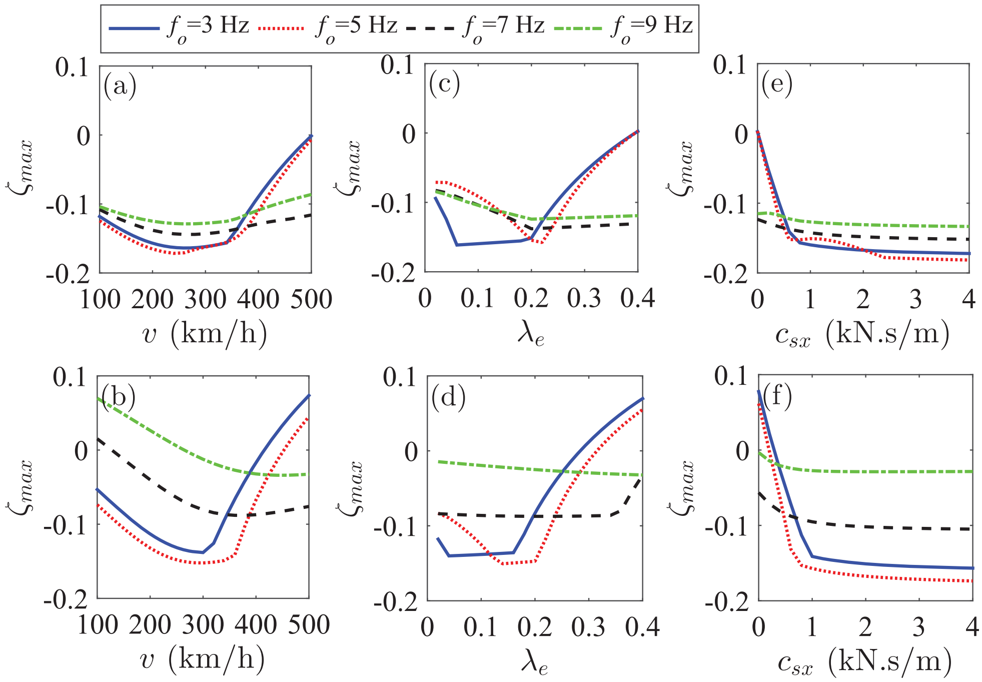

Figure 8. The linear system stability index with different parameters: (a) speed v, $\tau = 0$ ms; (b) speed v, $\tau = 15$ ms; (c) equivalent conicity λ_e, $\tau = 0$ ms; (d) equivalent conicity λ_e, $\tau = 15$ ms; (e) yaw damper damping c_{sx}, $\tau = 0$ ms; (f) yaw damper damping c_{sx}, $\tau = 15$ ms.

parameters, the influences of the bogie dynamic parameters on the system stability, such as running speed v, wheel–rail equivalent conicity λ_e and yaw damper damping c_{sx}, are analysed. The oscillator mass of 10 kg and ξ_o of 0.5 are defined. The ζ_{set} in Equation (13) is used to obtain the control gains. Figure 8 shows the calculated maximum system damping ratio $\zeta_{\max}$ of the bogie control system with the changing of v, λ_e and c_{sx}, respectively. In each subgraph, the horizontal axis shows the varied dynamics parameter within a certain range, and the vertical axis is the $\zeta_{\max}$. Subgraphs (a), (c) and (e) are the results with a delay of 0 ms at f_o of 3, 5, 7 and 9 Hz. Subgraphs (b), (d) and (f) are the results with a delay of 10 ms.

Subgraphs (a) and (b) reflect the influence of running speed v on the $\zeta_{\max}$. The system is most stable at speeds in the range from 200 to 350 km/h, in particular f_o is 5 Hz. The $\zeta_{\max}$ changes slightly if the f_o is larger than 7 Hz, which signifies a strong robustness against the perturbation of v, but it is not suitable for the dynamics requirements of the train. In subgraphs (c) and (d), just like v, if the f_o is smaller than or equal to 5 Hz, the effect of the λ_e on the $\zeta_{\max}$ is most favourable in a new wheel–rail contact state, in which the λ_e is between 0.1 and 0.2. Subgraphs (e) and (f) show the influence of the yaw damper damping c_{sx} on the system stability. The stability improves with the increase of c_{sx}, in particular the f_o is 5 Hz. We may thus conclude that the robustness of a control system with a large f_o is better than a system with a small f_o, but an appropriate f_o, such as 5 Hz, is conducive to the dynamics of the train. When a delay of 15 ms is considered, the stability of the system with a large f_o will worsen significantly.

5. State feedback of the oscillator

The root loci of the bogie under frame lateral vibration control based on the state feedback of an additional oscillator at different running speeds are studied to analyse the state feedback mechanism of the additional oscillator. The feedback gains are selected based on the ζ_{set} in Equation (13). Figure 9 shows the root loci of the system with different oscillator suspension parameters and time delay in the control system. Each root locus is composed of 30 sets of characteristic roots in the speed range from 20 to 600 km/h and each '+' indicates the corresponding mode information. A larger symbol represents a larger running speed. The horizontal axis indicates the mode damping ratio ζ (a negative sign indicates a stable value), which is the ratio of the real part to the modulus of eigenvalues of the matrix $\mathbf{A}_{cl}$ defined in Equation (10). The vertical axis indicates the damped vibration frequency, which is the imaginary part of the eigenvalues. Typically, as the speed increases, the damping of the hunting-related mode reduces. When the ζ is greater than 0, the hunting movement is unstable. In most cases, the low-frequency hunting mode determines the bogie hunting critical speed.

The CTA method is used to extend the dimension of the original system matrix. Compared to the system without delay, the time delay system has a greater number of vibration modes with a large damping ratio, but the large damping ratio does not affect the system dynamic performances. Additionally, the time delay affects the damping ratio of the low-frequency hunting mode, in turn affecting the system stability.

In Figure 9, subgraph (a) shows the results after applying control, in which the time delay τ is 0 ms and the oscillator parameters f_o and ξ_o are 5 Hz and 0.5, respectively. Subgraph

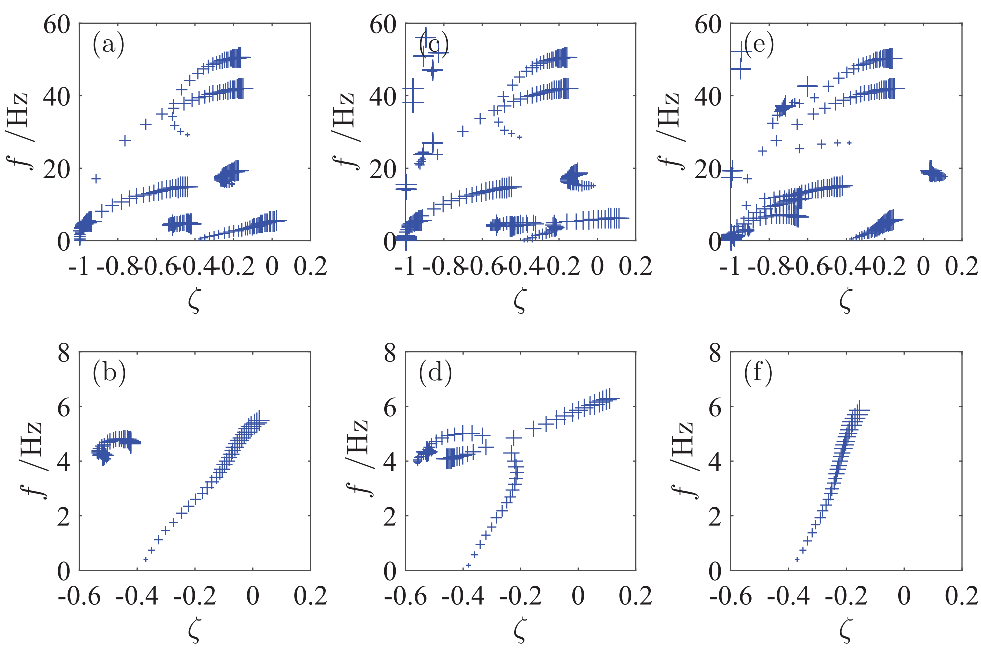

Figure 9. The root locus of the bogie control system in different calculation conditions: (a) $f_o = 5$ Hz, $\xi_o = 0.5$, $\tau = 0$ ms; (b) enlarged view of (a); (c) $f_o = 5$ Hz, $\xi_o = 0.5$, $\tau = 15$ ms; (d) enlarged view of (c); (e) $f_o = 9$ Hz, $\xi_o = 0.9$, $\tau = 15$ ms; (f) enlarged view of (e).

(b) shows the partial enlarged view of the low-frequency hunting mode. The bogie linear critical speed is 520 km/h under this calculation condition. Subgraph (c) shows the results of the bogie control system, in which the time delay τ is 15 ms and the f_o and ξ_o are 5 Hz and 0.5, respectively. Subgraph (d) is the partially enlarged view of subgraph (c), which shows that the critical speed is 460 km/h. Compared with subgraph (b), the bogie hunting stability improves significantly in the low- to mid-speed range, in which the hunting frequency is close to the oscillator natural frequency. However, it reduces in the high-speed range when the delay is considered. The damping ratio of the frame lateral vibration mode, of which the frequency is about 20 Hz, determines the system stability margin in low-speed range. This mode damping reduces especially at low speed due to the time delay. This is the reason for which the improvement of system stability caused by time delay in the low-speed range is not significant. Subgraph (e) shows the results of the bogie control system, in which the delay τ is 15 ms, and the f_o and ξ_o are 9 Hz and 0.9, respectively. Using the harder suspension is equivalent to feeding the state of frame back directly. Subgraph (f) is the partial enlarged view of subgraph (e). Compared with the subgraph (d), the bogie hunting stability improves especially in the high-speed range. However, the mode damping ratio of the frame lateral vibration is larger than 0, which signifies the instability of the control system. This instability is caused by the combination of a hard oscillator suspension and time delay in the control system.

In summary, the active control efforts can suppress the structure vibration, of which the frequencies are the same as the frequencies of the control efforts and feedback states. When an additional oscillator is used to provide the feedback states, the structure vibration of the oscillator response frequencies will be significantly weakened. The delay in the control system will affect the phase of the active actuator outputs, thus affecting the effects of vibration control. In this bogie control system, a delay of more than 20 ms reduces the bogie hunting stability at high speed. At the same time, it also helps to improve the bogie hunting stability within a certain speed range, in which the hunting frequency is close to the oscillator damped frequency, as shown in subgraph (d). In addition, the harder oscillator suspension is conductive to feeding the frame states back synchronously, thus suppressing the hunting movement and improving the bogie running stability more effectively, as shown in subgraph (f). However, the harder oscillator suspension will lead to instability of the control system at a certain time delay easily. Therefore, the improvement of bogie hunting stability and the reduction of control system stability must be considered when we optimising the oscillator parameters.

6. Non-linear stability analysis

A railway vehicle is a typical non-linear dynamic system, which is mainly reflected in the non-linear characteristics of the wheel–rail contact relationship and the suspension elements. The non-linearity of wheel–rail contact includes the wheel–rail contact geometry and saturation of wheel–rail creep force. In this study, a non-linear bogie lateral dynamics model was established, and the non-linear bifurcation of the bogie hunting under the frame vibration control was analysed using a direct integral method. The non-linear characteristics of wheel–rail contact geometry and creep saturation are considered in the bogie non-linear dynamics model. Based on a previous linear dynamics model, the wheel–rail contact equivalent conicity λ_e' can be expressed by a polynomial which is a non-linear function of the wheelset lateral displacement y_w. The polynomial and λ'_e at different wheelset lateral displacement are shown in reference [21]. Shen's method [27] was adopted to calculate the wheel–rail non-linear creep force.

According to the results of the linear stability analysis, the control system with a hard oscillator suspension stiffness is shown to have a strong robustness. The maximum damping ratio $\zeta_{\max}$ of the bogie system is close to the ζ_{set} in Equation (13), regardless of how fast the bogie running speed is. Therefore, the bogie hunting non-linear bifurcation does not exist under these calculation conditions. However, the time delay over 10 ms will lead to instability in the control system. In this section, the non-linear model was simulated to verify the linear system analysis. Figure 10 shows the wheelset lateral displacement curves of the bogie non-linear model under different parameter conditions. The bogie running speed is 350 km/h in the time domain simulation. Subgraph (a) shows the results before applying the active control with and without the fault of c_{sx}, respectively. It can be observed that the hunting of bogie with the fault of c_{sx} is unstable at this speed. Subgraph (b) shows the results after applying the active control with the delay of 0 and 15 ms, respectively. The oscillator suspension parameters f_o of 5 Hz and ξ_o of 0.5, as well as the fault of c_{sx}, are used. The results show that the frame vibration control can significantly improve the bogie hunting stability, and the convergence velocity of the wheelset lateral displacement is close to the non-fault system when the delay is not considered. At the same time, the delay of 15 ms worsens the bogie hunting stability significantly. Subgraph (c) shows the results after applying active control with the delay of 15 ms. The f_o of 9 Hz and ξ_o of 0.9, as well as the fault of c_{sx}, are used. It can be observed that the delay of 15 ms and hard oscillator suspension parameters render the control system unstable.

The bogie hunting bifurcation can be obtained using the direct integration of the non-linear model with a group of changed initial values, which is an approximate periodic solution and was calculated by numerical integration. Figure 11 shows the bifurcation curves of the wheelset lateral displacement versus the running speed under different conditions. The blue points in the figure represent the stable limit cycles, and the red points represent the unstable limit cycles. For the new wheel–rail contact, the bogie hunting has a typical subcritical bifurcation in all cases. The corresponding speed of a point where its vertical coordinate equals 0 is known as the linear critical speed, and the minimum speed of the unstable limit cycle is the non-linear critical speed.

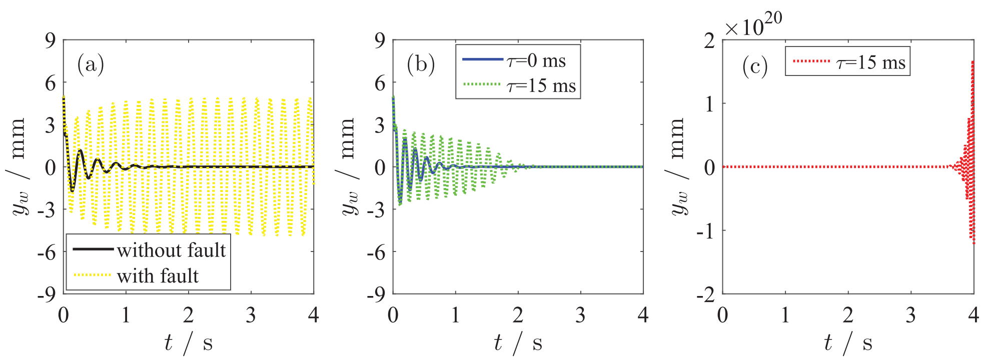

Figure 10. Wheelset lateral displacements in time domain with different system parameters: (a) uncontrolled; (b) $f_o = 5$ Hz, $\xi_o = 0.5$; (c) $f_o = 9$ Hz, $\xi_o = 0.9$, $\tau = 15$ ms.

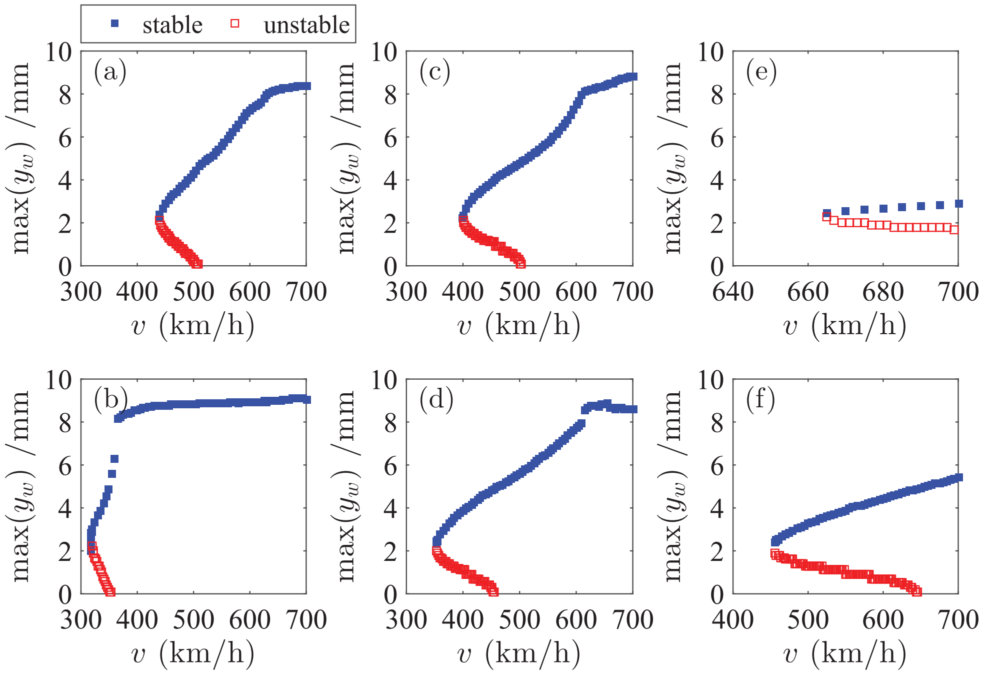

Figure 11. The wheelset lateral displacement bifurcation curves versus the running speed: (a) uncontrolled, without fault; (b) uncontrolled, with fault of c_{sx}; (c) $f_o = 5$ Hz, $\xi_o = 0.5$, $\tau = 0$ ms; (d) $f_o = 5$ Hz, $\xi_o = 0.5$, $\tau = 15$ ms; (e) $f_o = 7$ Hz, $\xi_o = 0.5$, $\tau = 0$ ms; (f) $f_o = 7$ Hz, $\xi_o = 0.5$, $\tau = 15$ ms.

Subgraphs (a) and (b) are the results before applying the active control with and without c_{sx} fault, respectively. The non-linear critical speeds are 420 and 310 km/h under the two conditions, respectively. With the fault of c_{sx}, the bogie non-linear critical speed cannot meet the requirement of running at the speed of 350 km/h. Subgraphs (c) and (d) are the results after applying the active control with the delay of 0 and 15 ms, respectively. The oscillator suspension parameters f_o of 5 Hz and ξ_o of 0.5, as well as the fault of c_{sx} are used. The non-linear critical speeds are 400 and 360 km/h under the two conditions, respectively. Subgraphs (e) and (f) are the results after applying the active control with the delay of 0 and 15 ms. The f_o of 9 Hz and ξ_o of 0.5, as well as the fault of c_{sx}, are used in this simulation. The non-linear critical speeds are 663 and 450 km/h in the two conditions, respectively. It can be seen that the bogie hunting stability improves significantly when a harder oscillator suspension is used. However, a harder oscillator suspension with time delay in the control system will cause system instability, as shown in Figure 10(c).

Based on the analysis of the linear system, the optimal oscillator suspension frequency f_o must be close to the bogie hunting frequency to improve the effects of active control. The bogie hunting frequency increases with the increasing of running speed. Therefore, the higher the bogie running speed is, the harder the oscillator suspension must be. A harder oscillator suspension is used to improve the hunting critical speed margin of the bogie control system. This requires for a variable stiffness for the oscillator suspension, since the train runs in a range of speeds.

7. Conclusion

(1) In this study, a method for frame lateral vibration control in high-speed train bogie was proposed to improve the hunting stability. Two inertial actuators are respectively mounted onto the front- and rear end beams of the frame, to exert the lateral active control efforts, thus controlling the lateral vibration of the frame. The actuator outputs are calculated by the linear state negative feedback of the states of two additional oscillators fixed on the beams. The displacements of the oscillator relative to the frame and the absolute velocity of the oscillator are taken as the state feedback. The multi-objective optimisation method (MOOP), with two objective functions of the stability index, as well as the control effort were solved using the NSGA-II algorithm leading to optimal feedback gains.

(2) The frame lateral vibration control can effectively improve the bogie hunting stability, according to the linear and nonlinear analysis of a high-speed bogie, in which a fault of the yaw damper and time delay in the control system are considered. The oscillator parameters have important implications on the bogie hunting stability. A large oscillator mass is conducive to the system stability and also adds more weight. The active control can suppress the structural vibration, and is efficient when the frequencies of the structural vibration and oscillator match, as expected. Therefore, the damped vibration frequency of the oscillator should be close to the bogie hunting frequency. The faster the bogie runs, the larger the oscillator suspension frequency must be. For the bogie in this study, the optimal values of the mass, natural frequency and damping ratio of the oscillator are found to be 10 kg, 5 Hz and 0.5, respectively, for the operating speed of 350 km/h.

(3) The effects of time delay in the control system on linear system stability are analysed using the CTA method. The time delay in the control system affects the phase of the active control output and worsens the system performance. In this study, it was observed that a delay of greater than 10 ms reduces the bogie hunting stability, especially when a hard oscillator suspension is used. However, it was also found that the robustness of the control against the perturbations of the system parameters with a hard oscillator suspension is better than the system with a soft one, and that an appropriate oscillator suspension with a damped frequency such as 5 Hz is conducive to the dynamics. Clearly, the time delay is important and must be considered in the multi-objective optimal design of the control.

Acknowledgments

The first author would like to thank the China Scholarship Council (CSC) for sponsoring his study in the USA.

Disclosure statement

No potential conflict of interest was reported by the authors.

Funding

The material in this paper is based on work supported by grants [51675443, 51735012, 11172197 and 11332008] from the National Natural Science Foundation of China, Sichuan Science and Technology Program [grant 2018JY0209], Research Innovation Team grant [17TD0040] of Sichuan Provincial University, and Traction Power State Key Laboratory [grant no. 2018TPL_T05, no. 2017TPL_T02] of the Independent Research and Development Projects.

References

[1] Goodall RM, Kortüm W. Mechatronic developments for railway vehicles of the future. Control Eng Pract. 2002;10(8):887–898.

[2] Ward CP, Weston PF, Stewart EJC, et al. Condition monitoring opportunities using vehicle-based sensors. Proc Inst Mech Eng F J. Rail Rapid Transit. 2011;225(2):202–218.

[3] Pearson JT, Goodall RM, Mei TX, et al. Active stability control strategies for a high speed bogie. Control Eng Pract. 2004;12(11):1381–1391.

[4] Abood KHA, Khan RA. Investigation to improve hunting stability of railway carriage using semi-active longitudinal primary stiffness suspension. J Mech Eng Res. 2010;2(5):97–105.

[5] Pearson JT, Goodall RM, Mei TX, et al. Design and experimental implementation of an active stability system for a high speed bogie. Veh Syst Dyn. 2004;41:43–52.

[6] Gretzschel M, Jaschinski A. Design of an active wheelset on a scaled roller rig. Veh Syst Dyn. 2004;41(5):365–381.

[7] Wickens AH. Comparative stability of bogie vehicles with passive and active guidance as influenced by friction and traction. Veh Syst Dyn. 2009;47(9):1137–1146.

[8] Perez J, Busturia JM, Goodall RM. Control strategies for active steering of bogie-based railway vehicles. Control Eng Pract. 2002;10(9):1005–1012.

[9] Wei X, Zhu M, Jia L. A semi-active control suspension system for railway vehicles with magnetorheological fluid dampers. Veh Syst Dyn. 2016;54(7):982–1003. Available from: http://dx.doi.org/10.1080/00423114.2016.1177189

[10] Ahmadian M, Mohan A. Semiactive control of hunting stability in rail vehicles. Proceedings of ASME International Mechanical Engineering Congress and Exposition (IMECE'05); 2005 Nov 5–11; Orlando, FL, USA; 2005. p. 63–68.

[11] Mei TX, Goodall RM. Recent development in active steering of railway vehicles. Veh Syst Dyn. 2003;39(6):415–436.

[12] Matamoros-Sanchez AZ, Goodall RM, Zolotas AC, et al. Stability control of a railway vehicle using absolute stiffness and inerters. Proceedings of 2012 UKACC International Conference on Control; 2012 Sept 3–5; Cardiff, UK; 2012. p. 120–127.

[13] Wang FC, Hsieh MR, Chen HJ. Stability and performance analysis of a full-train system with inerters. Veh Syst Dyn. 2012;50(4):545–571.

[14] Jiang JZ, Matamoros-Sanchez AZ, Goodall RM, et al. Passive suspensions incorporating inerters for railway vehicles. Veh Syst Dyn. 2012;50:263–276.

[15] Bruni S, Goodall R, Mei TX, et al. Control and monitoring for railway vehicle dynamics. Veh Syst Dyn. 2007;45(7–8):743–779.

[16] Alonso A, Giménez JG, Gomez E. Yaw damper modelling and its influence on railway dynamic stability. Veh Syst Dyn. 2011;49(9):1367–1387.

[17] Zhai W, Liu P, Lin J, et al. Experimental investigation on vibration behaviour of a crh train at speed of 350 km/h. Int J Rail Transp. 2015;3(1):1–16. Available from: http://dx.doi.org/10.1080/23248378.2014.992819

[18] Goodall RM, Bruni S, Mei TX. Concepts and prospects for actively controlled railway running gear. Veh Syst Dyn. 2006;44:60–70.

[19] Mei TX, Goodall RM. Stability control of railway bogies using absolute stiffness: sky-hook spring approach. Veh Syst Dyn. 2006;44:83–92.

[20] Zolotas AC, Pearson JT, Goodall RM. Modelling requirements for the design of active stability control strategies for a high speed bogie. Multibody Syst Dyn. 2006;15(1):51–66.

[21] Yao Y, Wu G, Sardahi Y, et al. Hunting stability analysis of high-speed train bogie under the frame lateral vibration active control. Veh Syst Dyn. 2017;1–22. Available from: http://dx.doi.org/10.1080/00423114.2017.1375128

[22] KA M, Azad I, Hasani SM. Vibration suppression of an underactuated dynamic system using virtual actuators. J Vibr Acoust. 2004;138(6):061006–061006–8. Available from: http://dx.doi.org/10.1115/1.4034082

[23] Yao Y, Zhang HJ, Luo SH. The mechanism of drive system flexible suspension and its application in locomotives. Transport. 2015;30(1):69–79.

[24] Yao Y, Zhang X, Liu X. The active control of the lateral movement of a motor suspended under a high-speed locomotive. Proc Inst Mech Eng F. 2015;230(6):1509–1520. 0954409715605138.
[25] Sun JQ. A method of continuous time approximation of delayed dynamical systems. Commun Nonlinear Sci Numer Simul. 2008;14(4):998–1007.
[26] Rifat S, Nejat O. Active vibration suppression with time delayed feedback. J Vibr Acoust. 2003;125(3):384–388.
[27] Shen ZY, Hedrick JK, Elkins JA. A comparison of alternative creep force models for rail vehicle dynamic analysis. Proceedings of 8th IAVSD Symposium on Vehicle System Dynamics, Dynamics of Vehicles on Roads and Tracks; 1983 Aug 15–19; MIT, Cambridge: Swets and Zeitlinger; 1984. p. 591–605.

Appendix

The matrices of the bogie system in Equation (1) are listed below.

$$
\mathbf{M}_b = \begin{bmatrix} m_w & & & & & & & \\ & I_w & & & & & & \\ & & m_w & & & & & \\ & & & I_w & & & & \\ & & & & m_f & & & \\ & & & & & I_f & & \\ & & & & & & m_o & \\ & & & & & & & m_o \end{bmatrix},
$$

$$
\mathbf{K}_b = \begin{bmatrix} 0 & & & & -k_{py} & -bk_{py} & & \\ & 0 & & & & -l_1^2 k_{px} & & \\ & & 0 & & -k_{py} & bk_{py} & & \\ & & & 0 & & -l_1^2 k_{px} & & \\ -k_{py} & & -k_{py} & & 2k_{py}+k_{sy}+2k_o & & -k_o & -k_o \\ -bk_{py} & -l_1^2 k_{px} & bk_{py} & -l_1^2 k_{px} & & \begin{matrix} l_2^2 k_{sx} + 2l_1^2 k_{px} \\ +2b^2 k_{py} + 2l_o^2 k_o \end{matrix} & -l_o k_o & l_o k_o \\ & & & & -k_o & -l_o k_o & k_o & \\ & & & & -k_o & l_o k_o & & k_o \end{bmatrix},
$$

$$
\mathbf{K}_r = \begin{bmatrix} k_{py}+k_{gy} & -2f_\eta & 0 & & \cdots & & 0 \\ \dfrac{2\lambda_e l_0 f_\zeta}{r_0} & l_1^2 k_{px}+k_{g\psi} & 0 & & \cdots & & 0 \\ 0 & 0 & k_{py}+k_{gy} & -2f_\eta & 0 & & 0 \\ & & \dfrac{2\lambda_e l_0 f_\zeta}{r_0} & l_1^2 k_{px}+k_{g\psi} & 0 & \cdots & 0 \\ \vdots & & 0 & 0 & 0 & & \\ & \vdots & \vdots & \vdots & & \ddots & \\ & & & & & & \ddots \\ 0 & & \cdots & \cdots & & & 0 \end{bmatrix},
$$

$$\mathbf{C}_b = \begin{bmatrix} 0 &&&&&&& \\ & 0 &&&&&& \\ && 0 &&&&& \\ &&& 0 &&&& \\ &&&& c_{sy} + 2c_o && -c_o & -c_o \\ &&&&& l_2^2 c_{sx} + l_o^2 c_o & -l_o c_o & l_o c_o \\ &&&& -c_o & -l_o c_o & c_o & \\ &&&& -c_o & l_o c_o && c_o \end{bmatrix},$$

$$\mathbf{C}_r = \begin{bmatrix} \frac{2f\eta}{v} &&&&&&& \\ & \frac{2l_0^2 f_\zeta}{v} &&&&&& \\ && \frac{2f\eta}{v} &&&&& \\ &&& \frac{2l_0^2 f_\zeta}{v} &&&& \\ &&&& 0 &&& \\ &&&&& 0 && \\ &&&&&& 0 & \\ &&&&&&& 0 \end{bmatrix},$$

$$\mathbf{E} = \begin{bmatrix} 0 & 0 & 0 & 0 & 1 & l_e & 0 & 0 \\ 0 & 0 & 0 & 0 & 1 & -l_e & 0 & 0 \end{bmatrix}^{\mathrm{T}},$$

$$\mathbf{D} = \begin{bmatrix} -1 & -L_o & 1 &&&&& \\ -1 & L_o && 1 &&&& \\ &&&& 0 & 0 & 1 & \\ &&&&&&& 1 \end{bmatrix}.$$